Electronic Supplementary Material (ESI) for Physical Chemistry Chemical Physics.

Electronic Supplementary Information

A New NMR Crystallographic Approach to Reveal the Calcium Local Structure of Atorvastatin Calcium

Sean T. Holmes,[‡, †,a] *Wei D. Wang,*[‡,b] *Guangjin Hou,*[†,a] *Cecil Dybowski,*[a] *Wei Wang,*[*, b]*and Shi Bai*[*,a, b]
[b]Department of Chemistry and Biochemistry, University of Delaware, Newark, Delaware 19716, USA
[b]State Key Laboratory of Applied Organic Chemistry, Lanzhou University, Lanzhou, Gansu, 730000, China

Corresponding Authors
*bais@udel.edu (S.B.); wang_wei@lzu.edu.cn (W.W.)

Table of Contents

Characterization of ATC-I

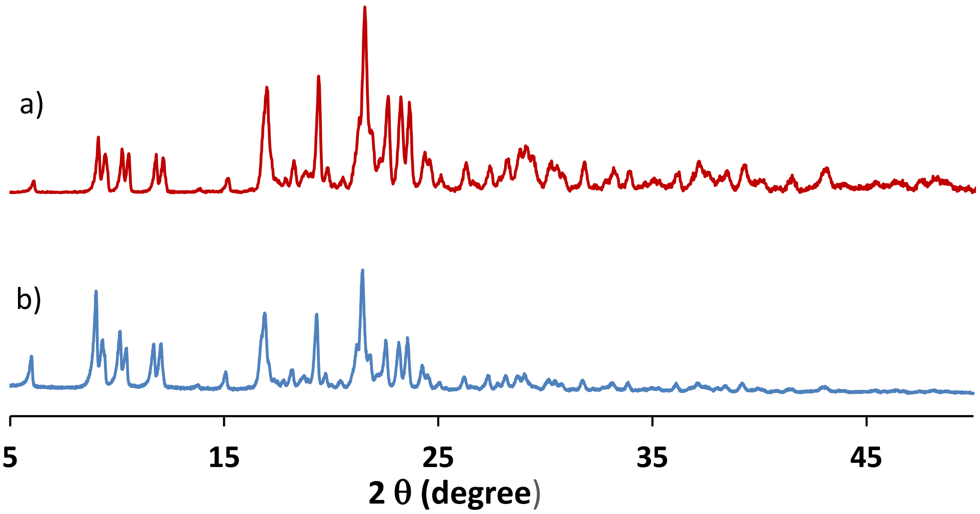

Fig. S1. PXRD patterns of ATC-I (b) and the ^{43}Ca enriched (62.2%) ATC-I (a).

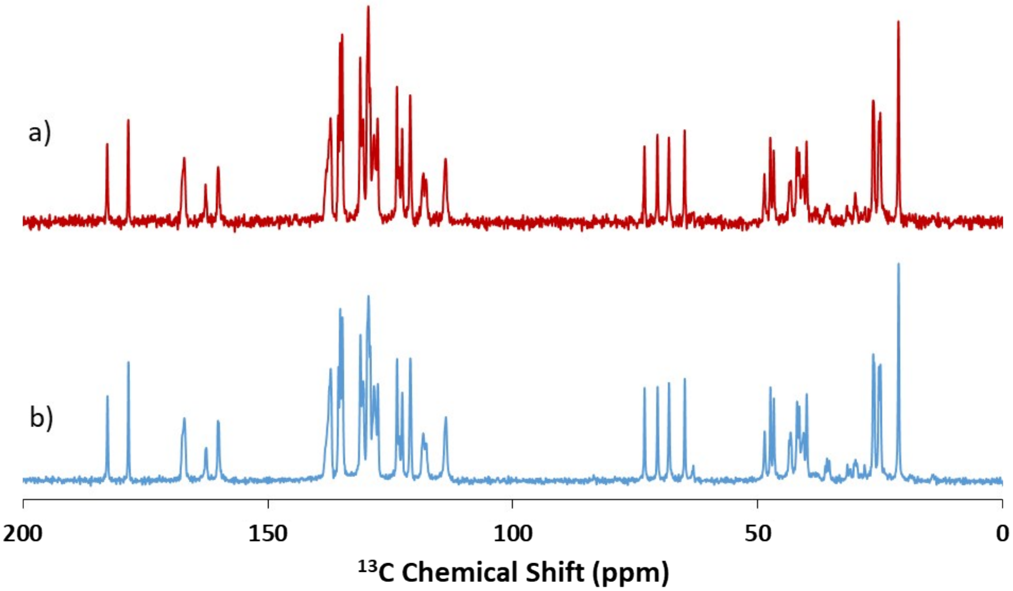

Fig. S2. ^{13}C CP/MAS NMR spectra of ATC-I (b) and the ^{43}Ca enriched (62.2%) ATC-I (a).

Statistical Analysis of NMR Parameters

The quadrupolar interaction characterizes the coupling between the nuclear quadrupole moment ($Q = -4.08$ fm^2) and the electric field gradient (EFG) at the nucleus. The parameters of importance are the quadrupole coupling constant ($C_Q = eQV_{33}/h$) and the asymmetry parameter, $\eta_Q = (V_{11} - V_{22})/V_{33}$. In these expressions, e is the elementary charge, h is Planck's constant, and V_{jj} (j = 1, 2, 3) refer to the principal values of the EFG tensor. One may equivalently describe the QC tensor by its principal components. Because the EFG tensor is traceless, only two principal components of the tensor are needed to describe the interaction.

All ^{43}Ca chemical shift tensors were converted to the chemical-shift scale using the expression:

$$\sigma_{ii} = A\delta_{ii} + B$$

In this model, σ_{jj} and δ_{jj} refer to the principal components of the calculated magnetic shielding and experimental chemical shift tensors, respectively. The best-fit parameters (HF/cc-pVDZ: $A = -1.00$, $B = 1250.4$; HF/cc-pVTZ: $A = -1.19$, $B = 1244.4$; PBE/cc-pVTZ: $A = -1.37$, $B = 1146.8$) were obtained from our previous investigations of ^{43}Ca chemical shifts in organic solids [Holmes, S.T.; Bai, S.; Iuliucci, R.J.; Mueller, K.T.; Dybowski, C., *J. Comput. Chem.*, **2017**, *38*, 949-956]. ^{13}C magnetic shielding was converted to the CS scale using the values reported in previous work [Sefzik, T.H.; Turco, D.; Iuliucci, R.J.; Facelli, J., *J. Phys. Chem. A*, **2005**, *109*, 1180-1187].

The quality of proposed model structures was assessed through reduced-χ statistics:

$$\chi_{CS} = \sqrt{\frac{1}{3}\sum_{jj}\left(\frac{\delta_{jj,exp} - \delta_{jj,calc}}{s_{CS}}\right)^2}$$

$$\chi_{EFG} = \sqrt{\frac{1}{2}\sum_{jj}\left(\frac{V_{jj,exp} - V_{jj,calc}}{s_{EFG}}\right)^2}$$

The values of the rms errors s_{CS} (HF/cc-pVDZ: 8.7 ppm; HF/cc-pVTZ: 6.2 ppm; PBE/cc-pVTZ: 11.2 ppm) and s_{EFG} (HF/cc-pVDZ: 0.17 MHz; HF/cc-pVTZ: 0.20 MHz; PBE/cc-pVTZ: 0.16 MHz) are taken from our previous work [Holmes *et al.*]. For the CS tensor, j = 1, 2, 3; for the EFG tensor, j = 1, 2.

Survey of Calcium-Containing Crystals in the Cambridge Structural Database

An up-to-date survey of the approximately 2800 calcium-containing compounds in the CSD has been carried out to search for a structure for the ^{43}Ca site in ATC-I. Since the calcium inner shell of ATC-I consists only of carboxylate and water ligands, the survey was restricted to crystal structures in which at least one of each of these ligands is coordinated with a calcium ion. Any structure containing transition metals, exhibiting errors, disorder, or without atomic coordinates deposited in the CSD was not considered. 103 calcium sites in 85 compounds with 14 distinct bonding arrangements (**Table S1**) meeting these criteria were identified (ignoring duplicate structures in the CSD arising from multiple independent measurements of the same material). The bonding motifs do not specify long-range interactions such as the sharing of the ligands between multiple calcium sites.

We made the general assumption that the calcium local structure of ATC-I belongs to one of the 14 structural motifs found in the CSD. However, some of the motifs in **Table S1** can be eliminated through further structural considerations. (1) Since the calcium-oxygen bonding motif in ATC-I must be consistent with an overall stoichiometry of $Ca(atorvastatin)_2{\cdot}3H_2O$, the structural motifs $Ca(COO)_6{\cdot}2H_2O$, $Ca(COO)_5{\cdot}2H_2O$, $Ca(COO){\cdot}6H_2O$, and $Ca(COO)_5{\cdot}H_2O$ were eliminated. (2) The survey of CSD indicated that carboxylate and water ligands in calcium salts were either fully coordinated with a single calcium site or shared between two calcium sites. Several structural motifs were eliminated if the bridging carboxylate and water ligands between calcium ions necessary to achieve the correct stoichiometry is inconsistent with the local bonding arrangements listed in **Table S1**. For example, for $Ca(COO)_2{\cdot}4H_2O$ to be a suitable model for the local calcium environment in ATC-I, the structure must consist of two carboxylate ligands and three water molecules coordinated with one calcium site and an additional water molecule shared between two calcium sites. Although 11 calcium sites with the general bonding motif of $Ca(COO)_2{\cdot}4H_2O$ were found in the CSD, none exhibited the necessary combination of bridging and terminal ligands between calcium ions to be consistent with the stoichiometry of ATC-I. The motifs $Ca(COO)_2{\cdot}4H_2O$, $Ca(COO)_3{\cdot}5H_2O$, $Ca(COO)_4{\cdot}4H_2O$, and $Ca(COO)_2{\cdot}5H_2O$ were eliminated by the same consideration. (3) The motifs $Ca(COO)_4{\cdot}H_2O$, $Ca(COO)_2{\cdot}6H_2O$, and $Ca(COO)_2{\cdot}7H_2O$ were eliminated because their coordination numbers were 5, 10, and 11, respectively, inconsistent with the $\delta_{iso}(^{43}Ca)$ of ATC-I (15.0 ppm). Thus, only three [$Ca(COO)_4{\cdot}2H_2O$, $Ca(COO)_3{\cdot}4H_2O$, and $Ca(COO)_3{\cdot}3H_2O$] of the 14 motifs in **Table S1** were examined as possible models of the local calcium structure of ATC-I (**Fig. S3**). These three motifs are ranked as the first, second, and fifth, in terms of the number of occurrences in the CSD survey.

Table S1. List of Ca-O bonding motifs and the CSD codes for the corresponding structures.

Bonding motif	Occurrences	CSD Codes
$Ca(COO)_4\cdot 2H_2O$	36	AQSCAA, CACOCT10, CACYRD, CAMALD01, CASALA01, CEJLIM, CEVGUF, COLJES, DIFTOE, DUPWOB01 EMUVUE (2 sites), FEBDAS, GEZYOZ, GLYCAD (6 sites), JORJUV, ISEQIH, LGLUCA, MAYKAY, MAJQIX, MOMQIQ, NARTOR, RAJFAL, RIGTAD, SAJCID, SAZKAG, ATADUU, ATADUU01, SEZYOL, VALCAC, ZABZAG
$Ca(COO)_3\cdot 4H_2O$	15	CAFUMT, CALCLA, CALCLA01, CAMELLO, CATPAL, CATPAL01, CATPAL02, CATPAL03, FOCWAW, FUVCII, JEDCOK01, HIFLAJ, LIWZAT, MITBAS, MITBAS01, RAVNAE, UTUQAC, SIRPOZ, OWEZEW
$Ca(COO)_2\cdot 4H_2O$	11	DODKIR, EMIPOF, EXOSAM (2 sites), HEDQEO (2 sites), LUQQIY, QUZWUE, ATADUU, ATADUU01, VINYAT, WAKCIX
$Ca(COO)_5\cdot H_2O$	10	CAGLCL, CAPHTH, FUJSAE01, GETTIJ, GEZYOZ, KOYSIC, KOYSOI, KOYTID, RUFMUA01, YOQYEK
$Ca(COO)_3\cdot 3H_2O$	9	AQUYUH, CAMELL10, CANAGL01, CANAGL10, CAVLOC, FEBDAS, GIFXAW, GLYCAD, THACCA, VAJYEK
$Ca(COO)\cdot 6H_2O$	6	BUYNUF, OPAWUY, SOZPEE, UTUREH (2 sites), CAHPAL10
$Ca(COO)_5\cdot 2H_2O$	4	CAMALD02, CAMALD03, CANIAC, JETVAF, TGLCAI, TGLCAI10
$Ca(COO)_4\cdot H_2O$	3	RAJFAL, SEZYOL, SOCFUM
$Ca(COO)_2\cdot 5H_2O$	2	EGIMIR, MISZUJ
$Ca(COO)_2\cdot 6H_2O$	2	ASEQAS, MOYVUS
$Ca(COO)_4\cdot 4H_2O$	2	GIFXAW, SEFHIW
$Ca(COO)_3\cdot 5H_2O$	1	TADJEQ
$Ca(COO)_6\cdot 2H_2O$	1	CAOXAL
$Ca(COO)_2\cdot 7H_2O$	1	GONTEK

Table S2. Experimental ^{43}Ca NMR parameters[a] for ATC-I, and calculated values for model structures. Calculated values were obtained for the previously proposed structure[b] and for the optimized model clusters representing the three bonding motifs.[c,d]

	δ_{iso} (ppm)	$\Delta\delta$ (ppm)	η_{CSA} (ppm)	C_Q (MHz)	η_Q	α (°)	β (°)	γ (°)
Experiment	**15.0(1)**	**-27(2)**	**0.50(20)**	**1.81(15)**	**0.44(13)**	**58(3)**	**5(3)**	**27(3)**
m1	-35.7	-10.0	0.36	-0.65	0.86	46	85	139
m2	-26.3	17.5	0.28	1.62	0.89	155	11	65
m3	-37.2	-21.9	0.74	-1.70	0.64	65	88	0
Previous structure	-21.5	22.8	0.57	-1.68	0.57	99	88	151

[a] The experimental uncertainty in the last digit(s) for each value is indicated in parentheses

[b] In the previous structure, the calcium environment was based on the structure of CBT

[c] Structures representing the three bonding motifs were fully optimized at the HF/cc-pVDZ level

[d] All calculations of ^{43}Ca NMR parameters were performed at the HF/cc-pVTZ level.

Table S3. List of top sixteen model structures of ATC-I, with χ_{CS}, χ_{EFG}, and β. The only structure matching experiment is denoted m3_140[a].

Structure Code	Model Chemistry	χ_{CS}	χ_{EFG}	β (deg.)	Structure Code	Model Chemistry	χ_{CS}	χ_{EFG}	β (deg.)
m1_54	HF	1.3	1.6	87.4	m3_10	HF	1.2	1.5	81.2
	PBE	0.9	1.0	89.4		PBE	0.7	0.8	70.6
m1_55	HF	1.2	1.8	86.4	m3_20	HF	1.1	1.3	56.3
	PBE	0.8	1.2	80.7		PBE	0.7	1.9	54.3
m1_78	HF	1.6	1.4	82.2	m3_115	HF	1.2	0.4	79.7
	PBE	1.1	1.3	80.7		PBE	0.4	0.9	78.1
m1_138	HF	1.0	1.7	89.1	m3_139	HF	1.5	1.6	72.4
	PBE	0.6	1.5	88.7		PBE	1.1	1.4	69.9
m1_224	HF	1.5	1.5	86.7	***m3_140***	**HF**	**0.6**	**1.2**	**9.4**
	PBE	0.7	1.7	86.6		**PBE**	**0.7**	**1.4**	**12.9**
m1_225	HF	1.2	0.9	84.9	m3_141	HF	0.9	1.1	78.5
	PBE	0.6	0.2	87.6		PBE	0.9	1.3	77.2
m3_5	HF	1.4	1.4	9.9	m3_157	HF	1.4	0.7	22.2
	PBE	0.8	0.8	32.5		PBE	0.9	1.6	22.2
m3_9	HF	1.2	1.5	80.4	m3_158	HF	0.5	0.9	89.3
	PBE	0.7	0.8	69.7		PBE	0.2	0.8	88.8

[a] In the structure code of m3_140, m3 represent the motif III and 140 is the entry number of the structure generated in this motif. This notation is also applicable to other structure codes. The *m3_140* was highlighted for clarity.

Analysis of Relative Orientations of EFG and CSA Tensors Based on ^{43}Ca Local Symmetry

We review all possibilities of crystal symmetry that have an effect on the relative orientations of the EFG and CSA tensors of a ^{43}Ca nucleus by first defining the following notation: the principal axes of the EFG tensor are x_Q, y_Q, z_Q and the principal axes of the CSA tensor are x_C, y_C, z_C. No distinction is made between positive and negative axes because the NMR spectrum is not affected by it. The three Euler angles defining the orientation of the EFG tensor relative to the CSA tensor are α, β, γ. Since we ignore the difference between positive and negative axis directions, the ranges of the parameters are $0° \leq \alpha \leq 180°$, $0° \leq \beta \leq 90°$, $0° \leq \gamma \leq 180°$. If one EFG axis coincides with a CS axis, the principal axes of the two systems in the perpendicular plane are oriented with respect to each other by an angle ψ, which can be restricted to $0° \leq \psi \leq 90°$ if we ignore the difference between positive and negative axis directions.

If a two-fold symmetry axis, C_2, passes through the position of the calcium site, then one of the principal axes of both the EFG and the CS tensors must coincide with the symmetry axis. Consequently, one of the CS principal axes must be parallel to one of the QC principal axes, whereas the other axes two axes are related by an angle ψ. **Table S4** lists the nine possibilities of such relative orientations and the corresponding nine consequences for the Euler angles ($\Sigma \equiv C_2$). Special cases when ψ is 0° or 90°, such that three pairs of axes coincide, are not explicitly included here and are reviewed separately below. Note that a two-fold symmetry axis does not impose symmetry on the interaction tensors.

If the calcium site is located on a mirror plane, then one of the principal axes of both the EFG and the CS tensors will point in a direction Σ perpendicular to the mirror plane. Consequently, one of the CS axes is parallel to one of the EFG axes, whereas the other axes are again related by the angle ψ. The nine possibilities are identical to the two-fold symmetry axis case and are, therefore, also listed in **Table S4**. Note that a mirror plane does not impose symmetry on the interaction tensors.

In a situation in which the calcium site is simultaneously located on one of the following pairs of symmetry elements: (1) two C_2 axes that are perpendicular to each other, (2) two mirror planes that are perpendicular to each other (C_{2v} point group symmetry), or (3) a mirror plane and a C_2 axis that lies in the mirror plane (C_{2v} point group symmetry), two principal QC principal axes coincide with two CS principal axes, which requires the third axis pair to coincide as well. In such a case there are six ways in which the axis systems can coincide (**Table S5**). Addition of more two-fold axes or mirror planes to one of the three mentioned double occurrences does not restrict the relations between the two tensor orientations further. In summary, a C_{2v} symmetry point group is expected for the calcium site for these cases.

If the nucleus Ca is located on a symmetry axis of order 3 or higher, then the interaction tensors must be axially symmetric ($\eta_{CSA} = \eta_Q = 0$) and the two principal axes coincide and are usually labeled the *z* axis. The Euler angle β is zero in this situation, and there is no restriction at all on the angles α and γ because a rotation about the symmetry *z* axis is irrelevant.

The Euler angles (α, β, γ) of the calcium site in ATC-1 are experimentally determined to be 58(± 3)°, 5(±3)°, and 27(±3)°. β (5°) and $\alpha + \gamma$ (85°) are close within experimental error to the cases in which β = 0° and $\alpha + \gamma$ = 90°, or cases 1 and 3. The 33 principal axes of the EFG and CS interactions are collinear while the other principal axes are also nearly coaxial ($\alpha + \gamma$ = 180°, 90°or 270°) with specification of relatedness. For all other cases (2, 4, 5, and 6, the 33 principal axes of the QC and CS interactions are perpendicular to each other (β = 90°).

Although all cases in **Table S5** belong to the same point group C_{2v}, SIMPSON simulations (**Fig. S4**) using the experimentally determined CS and QC interactions showed that the ^{43}Ca line shape is the same for each case, while the line shapes of cases 1 and 3 in which β = 0° are nearly identical. Although one cannot distinguish symmetry cases 1 and 3 though the analysis of ^{43}Ca NMR line shape, the special feature of the experimental and simulated line shapes revealed that calcium site in ATC-I possess a local symmetry of C_{2v}.

SIMPSON simulations (at 11.75 T and 19.97 T) demonstrate that, as long as $\alpha + \gamma$ is kept close to 90° and β is close to 0 (cases 1 and 3), the ^{43}Ca NMR line shapes are nearly identical (**Fig. S5**) regardless what individual α and γ values are chosen, consistent with the symmetry analysis given in **Table S5**. In addition, as long as β is close to 0, very little impact of the ($\alpha + \gamma$) value on ^{43}Ca line shape is observed (**Fig. S6**).

The impact of β on the ^{43}Ca line shape in ATC-I, however, is significant at both 11.75 T and 19.97 T. The sharp feature in the simulated spectrum with β of 0° and 5° becomes less intense or disappears in the simulated spectrum with β = 20° or more, particular at 19.97 T. A 5-degree change in β, when β > 5°, causes obvious changes in line shape (**Fig. S7**).

In summary, the calcium site symmetry analysis and the ^{43}Ca line-shape simulation demonstrate that (1) the calcium site in ATC-I has a local symmetry approaching the group point C_{2v} and (2) while α and γ have little impact, β is very sensitive to the ^{43}Ca line shape and, thus, can be used as a unique benchmark for screening the candidate structures.

Table S4. The nine possibilities and the corresponding Euler angles when one principal-axis direction of the EFG tensor and also of the CSA tensor coincides with a unique symmetry direction Σ. When two options are listed for an Euler angle, both are possible based on the angle ranges specified above.

coincident axes	α	β	γ	angle between axes
$\Sigma // x_Q // x_C$	90°	ψ	90°	$\psi = \angle(z_Q, z_C)$
$\Sigma // x_Q // y_C$	0°, 180°	ψ	90°	$\psi = \angle(z_Q, z_C)$
$\Sigma // x_Q // z_C$	ψ	90°	0°, 180°	$\psi = \angle(y_Q, y_C)$
$\Sigma // y_Q // x_C$	90°	ψ	0°, 180°	$\psi = \angle(z_Q, z_C)$
$\Sigma // y_Q // y_C$	0°, 180°	ψ	0°, 180°	$\psi = \angle(z_Q, z_C)$
$\Sigma // y_Q // z_C$	90° ± ψ	90°	90°	$\psi = \angle(x_Q, x_C)$
$\Sigma // z_Q // x_C$	0°, 180°	90°	ψ	$\psi = \angle(y_Q, y_C)$
$\Sigma // z_Q // y_C$	90°	90°	90° ± ψ	$\psi = \angle(x_Q, x_C)$
$\Sigma // z_Q // z_C$	any α	0°	$\alpha + \gamma = \psi$, ψ + 180°	$\psi = \angle(x_Q, x_C)$

Table S5. The six possibilities when all three principal-axis directions of the EFG tensor coincide with CS tensor principal axes listed with the corresponding Euler angles. When two options are listed for an Euler angle, both are possible based on the angle ranges specified above.

case	(x_Q, y_Q, z_Q) coincide with	α	β	γ
1	(x_C, y_C, z_C)	any α	0°	$\alpha + \gamma$ = 180°
2	(x_C, z_C, y_C)	90°	90°	90°
3	(y_C, x_C, z_C)	any α	0°	$\alpha + \gamma$ = 90°, 270°
4	(y_C, z_C, x_C)	0°, 180°	90°	90°
5	(z_C, x_C, y_C)	90°	90°	0°, 180°
6	(z_C, y_C, x_C)	0°, 180°	90°	0°, 180°

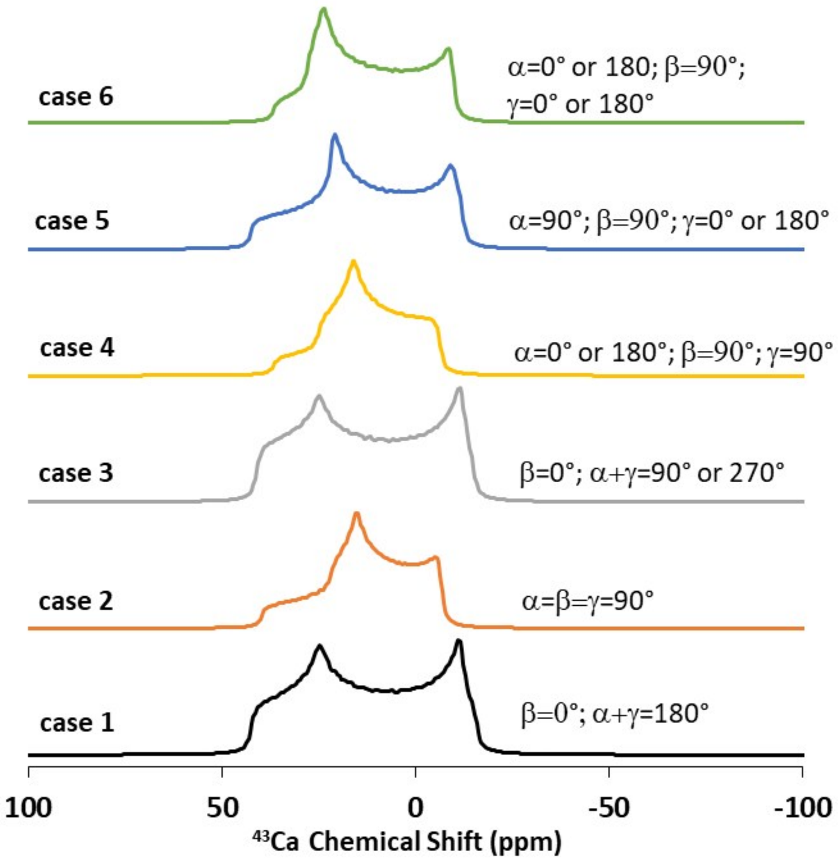

Fig. S3: SIMPSON simulation of six cases in Table S5. All CS and EFG tensor parameters used here are experimental values for ATC-I obtained at 19.97 T, the Euler angles are chosen according to the cases given in Table S5.

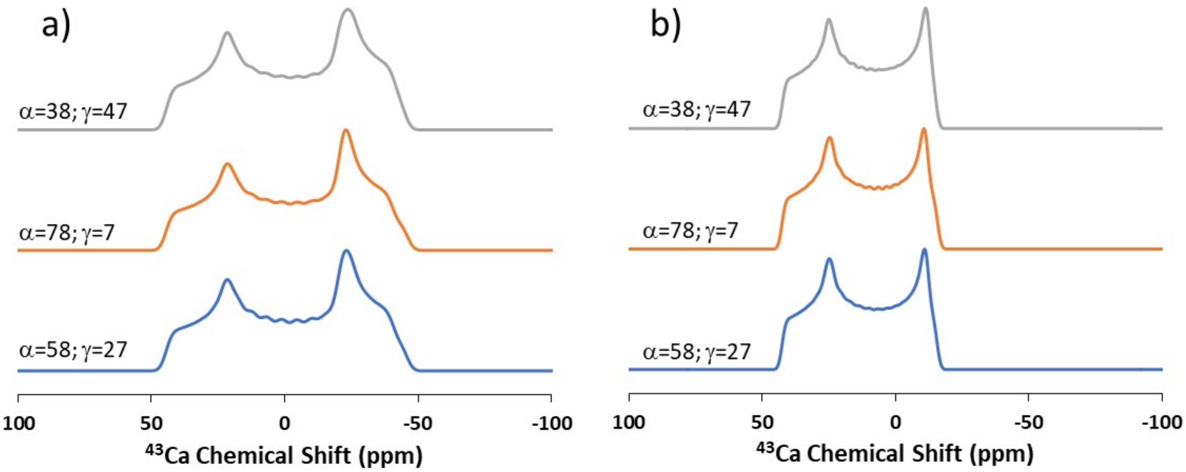

Fig. S4. SIMPSON simulations of ^{43}Ca line shape of ATC-I as a function of α and γ at 11.75 T (a) and 19.97 T (b). In these simulations, the sum of α and γ was kept as a constant (85° obtained experimentally) while α and γ were varied in a range of 40°. β was fixed as 5° for these simulations. No significant changes in ^{43}Ca lineshape were observed under the conditions of these simulations.

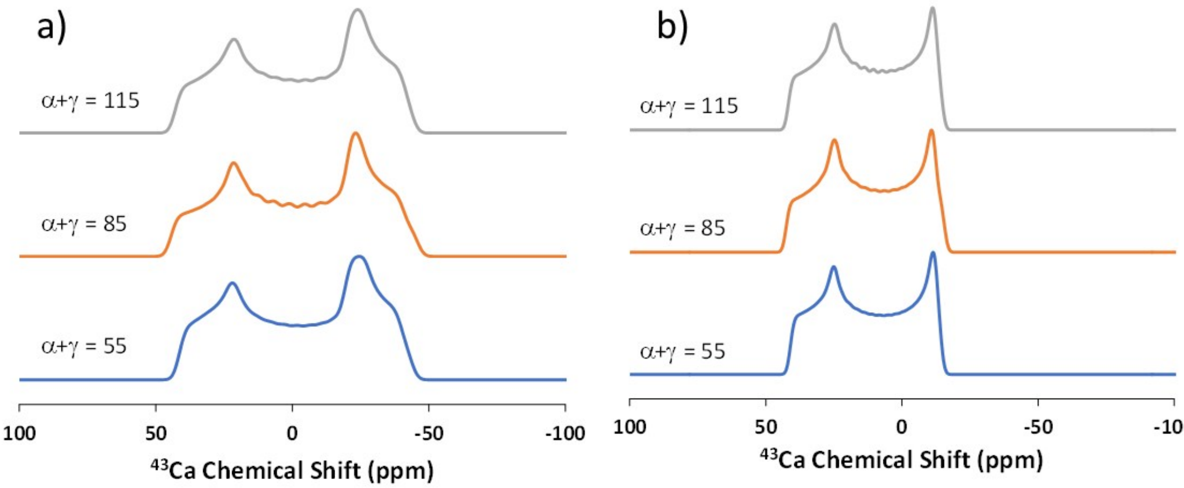

Fig. S5. SIMPSON simulations of ^{43}Ca line shape of ATC-I as a function of $(\alpha+\gamma)$ at 11.75 T (a) and 19.97 T (b). In these simulation, $(\alpha + \gamma)$ was varied from 55° to 115°. The simulation of $(\alpha + \gamma) = 85$° corresponds to the experimental ^{43}Ca SSNMR powder patterns. β was fixed as 5° for these simulations. No significant changes in ^{43}Ca line shape were observed under the conditions of these simulations.

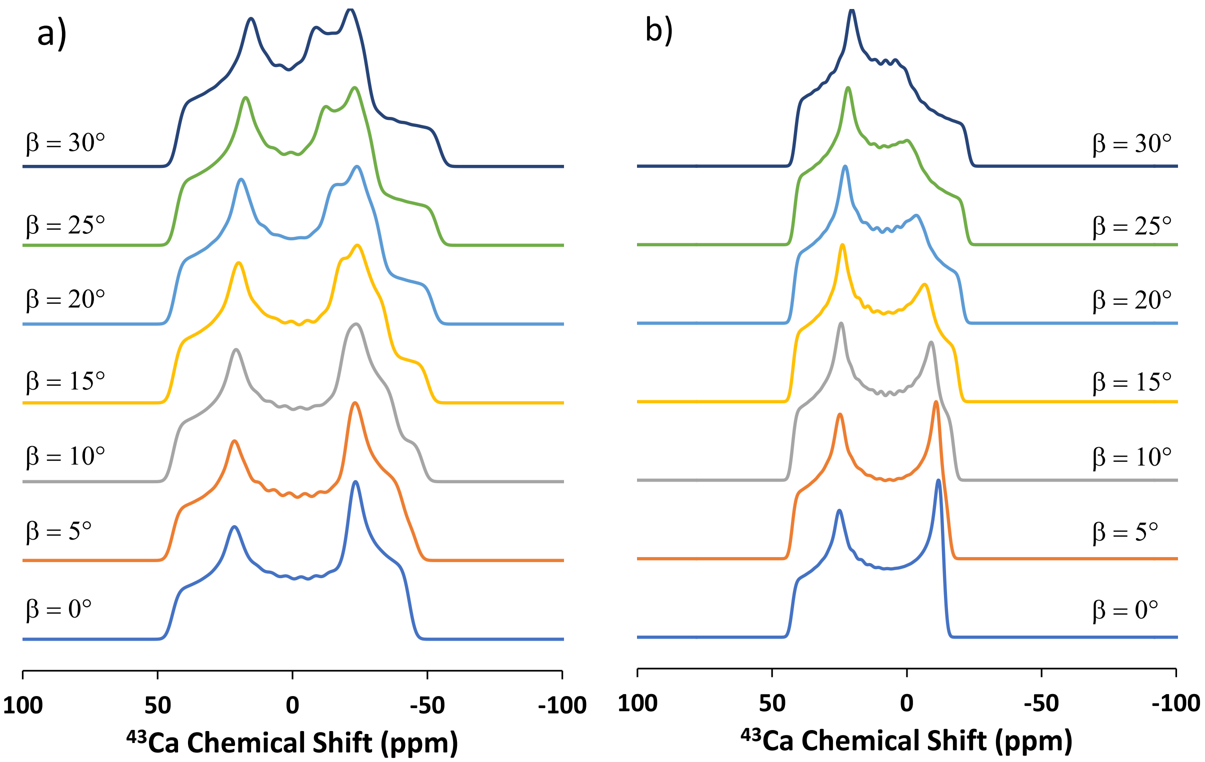

Fig. S6. Simulations of the ^{43}Ca ssNMR line shape with SIMPSON as a function of the Euler angle β the angle between V_{33} and δ_{33}, at 11.75 T (a) and 19.97 T (b). In these simulation, the values of α and γ, CS and QC parameters are taken from Table 1 for ATC-I. Significant change in line shape can be observed when β is increased to 10°.

Structural Analysis of *m3_140*

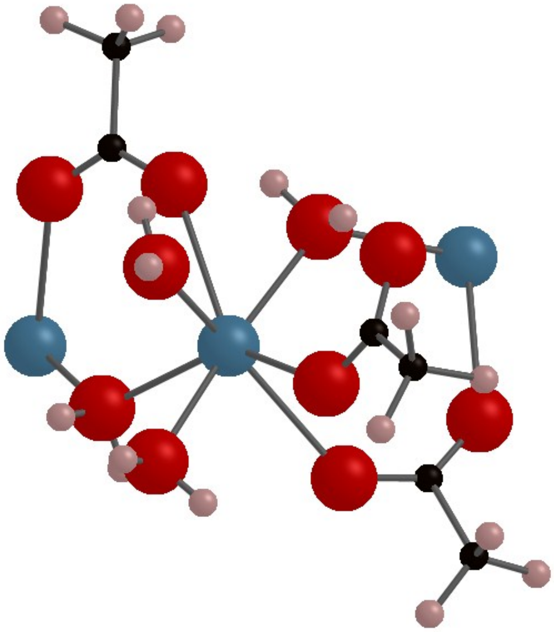

Fig. S7. Augmented *m3_140* structure: To evaluate the predicted ^{43}Ca NMR spectra, an augmented model cluster was constructed by inserting two additional calcium ions based on the assumption that two structurally similar atorvastatin ligands are each bound to two calcium ions. Placement of the additional calcium ions clearly revealed that two water ligands are also shared between two calcium sites. The positions of the hydrogen atoms in the augmented cluster of composition $[Ca_3(acet)_3 \cdot 4H_2O]^{3+}$ were refined at the HF/cc-pVDZ level. Previous multidimensional ssNMR studies of atorvastatin[1] revealed ^{13}C isotropic CSs of two carboxyl carbons in ATC-I, implying that there are two experimentally distinguishable carboxyl groups in the structure. The ^{13}C NMR calculation of this work showed that one ligand of the augmented *m3_140* structure is bound to a single calcium ion, whereas another ligand is shared between two calcium ions.

Table S6. Selected bond lengths and bond angles in *m3_140* for ATC-I.

First Ca-O contact (Å)	Second Ca-O contact (Å)	∠Ca-O-C (deg.)
2.63	3.96	131
2.66	4.08	141
2.31	3.48	127

Table S7. Experimental ^{13}C CS tensors in ATC-I and calculated ^{13}C CS tensors for the extended model (Fig. S4) representing ^{43}Ca local structure for ATC-I

Carboxylic carbons		δ_{iso} (ppm)	$\Delta\delta$ (ppm)	η_{CSA}
Ligand *a*	Exp.	178.5	-103	0.52
	HF	177.1	-122	0.53
Ligand *b*	Exp.	182.7	-120	0.4
	HF	182.3	-128	0.35

Atomic Coordinates of *m3_140*

Ca	0.00000	0.00000	0.00000
C	-0.89147	3.551096	-0.70748
C	1.882442	-2.16752	2.148276
C	-1.5213	-1.82518	2.172908
H	-0.46026	-2.45444	-1.37915
H	-2.2345	1.209111	-0.47288
H	-2.88486	-0.1766	-0.53216
H	-0.79484	0.781441	2.398664
H	-0.77512	2.035927	1.484444
O	-0.88641	2.510167	0.007189
O	1.573096	-1.8726	0.967289
O	-1.85524	-0.81709	2.831245
O	-0.32957	3.642487	-1.80079
O	1.949129	-1.40212	3.148164
O	-0.7102	-1.82327	1.227733
O	1.141717	0.544642	-2.14276
O	-0.04924	-1.62639	-1.60102
O	-2.05441	0.280248	-0.5921
O	-0.23655	1.34417	1.859794
C	-1.63676	4.746007	-0.15333
H	-1.65264	5.569515	-0.86455
H	-1.14983	5.07228	0.768289
H	-2.65753	4.456138	0.101238
C	-2.14028	-3.14628	2.5867
H	-3.22771	-3.04997	2.587736
H	-1.8335	-3.3808	3.608261
H	-1.8463	-3.96025	1.926266
C	2.147221	-3.63947	2.419553
H	2.828278	-3.77093	3.260089
H	2.538469	-4.14494	1.536888
H	1.192858	-4.10679	2.680881

Determination of the Calcium Environment in Calcium Acetate Monohydrate

Table S8. Experimental ^{43}Ca NMR parameters for calcium acetate·H_2O and calculated NMR parameters for five model structures[a]

Structure No.	Model Chemistry	δ_{11} (ppm)	δ_{22} (ppm)	δ_{33} (ppm)	χ_{CS}	C_Q (MHz)	η_Q	χ_{EFG}	β (deg.)
Exp.	**-**	**24.3**	**12.8**	**4.3**	**-**	**1.37**	**0.1**	**-**	**90**
1	HF	14.5	4.7	0.4	1.2	-1.11	0.33	0.9	88
	PBE	20.2	5.5	0	0.9	-0.95	0.08	1	66
2	HF	15.5	6.1	1.6	1.1	-1.18	0.73	1.9	87
	PBE	21.6	9.1	2.5	0.5	-1.06	0.69	1.7	69
3	HF	15.5	4.8	0.9	1.2	-1.24	0.64	1.7	87
	PBE	21.3	8	-0.2	0.7	-1.1	0.57	1.4	70
4	HF	14.4	2.3	-0.7	1.4	-1.2	0.28	0.7	88
	PBE	19.4	3.9	-4.1	1.2	-1.05	0.12	0.8	71
5	HF	16.1	4	-1.1	1.2	-1.18	0.37	0.9	87
	PBE	19.6	4.7	-2.6	1.1	-0.97	0.47	1.3	74

[a] The screening procedure followed the same steps used in the prediction of the structure of ATC-I. In the first stage of screening, the 999 structures were evaluated by calculation of ^{43}Ca CS and QC tensors at the HC/cc-pVDZ level. All but 21 (9, 4, and 8 model structures corresponding to m1, m2, and m3, respectively) structures were eliminated at this early stage. In the next screening stage, a geometry optimization was employed at the HF/cc-pVDZ level, followed by calculation of ^{43}Ca NMR parameters at the HF/cc-pVTZ level. Screening based on ^{43}Ca NMR parameters reduced the number of possible model structures to five. Calculation at the PBE/cc-pVTZ level did not eliminate any further structures. The five final structures all belong to motif I, consistent with the known single-crystal XRD structure, with ^{43}Ca NMR parameters provided in the Table. These five structures all have the similar β values, indicating they are similar in the symmetry near calcium site.